

# General Approach to Individually Dispersed, Highly Soluble, and Conductive Graphene Nanosheets Functionalized by Nitrene Chemistry

Hongkun He and Chao Gao\*

MOE Key Laboratory of Macromolecular Synthesis and Functionalization, Department of Polymer Science and Engineering, Zhejiang University, 38 Zheda Road, Hangzhou 310027, P. R. China

Received June 11, 2010. Revised Manuscript Received July 23, 2010

A unified approach to covalently functionalize graphene nanosheets based on nitrene chemistry is reported. This strategy is simple and efficient, allowing various functional moieties (e.g., hydroxyl, carboxyl, amino, bromine, long alkyl chain, etc.) and polymers (e.g., poly(ethylene glycol), polystyrene) to covalently and stably anchor on graphene to produce single-layer functionalized graphene from graphene oxide in a one-step reaction. The structure and morphology of nanosheets are characterized using microscopy (AFM, SEM, TEM), spectroscopy (FTIR, XPS, Raman), thermal gravimetric analysis (TGA), and X-ray diffraction (XRD) measurements. The resulting functionalized graphene nanosheets are electrically conductive, readily dispersible in solvents and easily processable, making them promising candidates for further modification and applications such as nanohybrids, and polymer composites, etc. The presented work provides a general methodology to prepare individually dispersed graphene nanosheets with various functionalizations and properties, paving the way for the synthesis and applications of functionalized graphene materials.

## Introduction

Graphene, the two-dimensional (2D) monolayer of carbon atoms arranged in honeycomb lattice, has received tremendous attention because of its remarkable properties and promising potential applications.<sup>1–4</sup> Although graphene is an ideal substrate that is suitable for some purposes, it contains rare surface functional moieties and very limited dispersibility in solvents, seriously limiting the exertion of its great potentials. Thus, developing chemical methods to functionalize graphene has become one of the most critical issues in the exploring of graphene technologies. It is expected that the chemical modification could not only enhance its solubilities and processabilities, but also render new properties to graphene and even greatly widen its application scope.<sup>5–15</sup>

Before diving into the functionalization of graphene, one pivotal question has to be clarified at first—how to obtain graphene? Since the discovery of graphene in 2004,<sup>16</sup> a number of studies concerning this issue have continuously appeared, which in general can be categorized into two main methods. One method is to directly generate graphene either by a top-down approach (e.g., mechanical cleavage of graphite<sup>17</sup>) or a bottom-up approach (e.g., organic synthesis,<sup>18</sup> epitaxial growth,<sup>19</sup> and chemical vapor deposition<sup>20</sup>). By using this method, one can produce relatively more perfect graphene with fewer defects, but the yield of the product is quite low. The other method is to first prepare graphene oxide (GO) by the oxidation of graphite with strong oxidants (using the previously reported oxidation approaches such as Hummers,<sup>21</sup> Staudenmaier,<sup>22</sup> or Brodie method<sup>23</sup>) and then convert GO to graphene by reduction via thermal, chemical, or electrochemical

\*Corresponding author. E-mail: chaogao@zju.edu.cn.

- (1) Geim, A. K.; Novoselov, K. S. *Nat. Mater.* **2007**, *6*, 183–191.
- (2) Rao, C. N. R.; Sood, A. K.; Subrahmanyam, K. S.; Govindaraj, A. *Angew. Chem., Int. Ed.* **2009**, *48*, 7752–7777.
- (3) Rao, C. N. R.; Sood, A. K.; Voggu, R.; Subrahmanyam, K. S. *J. Phys. Chem. Lett.* **2010**, *1*, 572–580.
- (4) Allen, M. J.; Tung, V. C.; Kaner, R. B. *Chem. Rev.* **2010**, *110*, 132–145.
- (5) Liu, Z.; Robinson, J. T.; Sun, X.; Dai, H. J. *Am. Chem. Soc.* **2008**, *130*, 10876–10877.
- (6) Park, S.; Ruoff, R. S. *Nat. Nanotechnol.* **2009**, *4*, 217–224.
- (7) Ruoff, R. S. *Nat. Nanotechnol.* **2008**, *3*, 10–11.
- (8) Geim, A. K. *Science* **2009**, *324*, 1530–1534.
- (9) Stankovich, S.; Piner, R. D.; Nguyen, S. T.; Ruoff, R. S. *Carbon* **2006**, *44*, 3342–3347.
- (10) Niyogi, S.; Bekyarova, E.; Itkis, M. E.; McWilliams, J. L.; Hamon, M. A.; Haddon, R. C. *J. Am. Chem. Soc.* **2006**, *128*, 7720–7721.
- (11) Wang, S.; Chia, P.; Chua, L.; Zhao, L.; Png, R.; Sivaramakrishnan, S.; Zhou, M.; Goh, R. G.; Friend, R. H.; Wee, A. T.; Ho, P. K. *Adv. Mater.* **2008**, *20*, 3440–3446.
- (12) Xu, Y.; Liu, Z.; Zhang, X.; Wang, Y.; Tian, J.; Huang, Y.; Ma, Y.; Zhang, X.; Chen, Y. *Adv. Mater.* **2009**, *21*, 1275–1279.
- (13) Bai, H.; Xu, Y.; Zhao, L.; Li, C.; Shi, G. *Chem. Commun.* **2009**, *45*, 1667–1669.
- (14) Li, X. L.; Wang, X. R.; Zhang, L.; Lee, S. W.; Dai, H. J. *Science* **2008**, *319*, 1229–1232.
- (15) Li, X.; Zhang, G.; Bai, X.; Sun, X.; Wang, X.; Wang, E.; Dai, H. *Nat. Nanotechnol.* **2008**, *3*, 538–542.
- (16) Novoselov, K. S.; Geim, A. K.; Morozov, S. V.; Jiang, D.; Zhang, Y.; Dubonos, S. V.; Grigorieva, I. V.; Firsov, A. A. *Science* **2004**, *306*, 666–669.
- (17) Geim, A. K.; Novoselov, K. S. *Nat. Mater.* **2007**, *6*, 183–191.
- (18) Wu, J. S.; Pisula, W.; Mullen, K. *Chem. Rev.* **2007**, *107*, 718–747.
- (19) Berger, C.; Song, Z. M.; Li, X. B.; Wu, X. S.; Brown, N.; Naud, C.; Mayou, D.; Li, T. B.; Hass, J.; Marchenkov, A. N.; Conrad, E. H.; First, P. N.; de Heer, W. A. *Science* **2006**, *312*, 1191–1196.
- (20) Kim, K. S.; Zhao, Y.; Jang, H.; Lee, S. Y.; Kim, J. M.; Kim, K. S.; Ahn, J.; Kim, P.; Choi, J.; Hong, B. H. *Nature* **2008**, *457*, 706–710.
- (21) Hummers, W. S.; Offeman, R. E. *J. Am. Chem. Soc.* **1958**, *80*, 1339–1339.
- (22) Staudenmaier, L. *Ber. Dtsch. Chem. Ges.* **1898**, *31*, 1481–1487.
- (23) Brodie, B. C. *Ann. Chim. Phys.* **1860**, *59*, 466–472.

techniques.<sup>24</sup> Although the graphene obtained by using the second method has a little more defects than that obtained by using the first method, its overall quality is sufficiently good resulting from the recovery of the conjugated network. More importantly, with GO as the starting material, graphene could be available in large quantities, paving the way for the scalable functionalization of graphene. Besides, GO has many oxygen-containing functional groups and are highly soluble in water. However, GO is electrically insulative, so in order to maintain the superior electrical property, GO has to be reduced to graphene. Also, the functional groups on GO are labile and would easily decompose when GO is heated at an elevated temperature or in the presence of reducing agents. Furthermore, there are a few kinds of functional groups (e.g., hydroxyl, carboxyl, and epoxy groups) on GO, which may cause trouble in its modification and characterization. Therefore, it is highly needed to find a method to introduce stable and specific functional moieties to graphene.

As for how to search for such methods to functionalize graphene, given that both graphene and carbon nanotubes (CNTs) consist of carbon atoms linked by  $sp^2$  bonds, it would be possible to functionalize graphene by the well-established methods for the functionalization of CNTs.<sup>25</sup> Indeed, some recent efforts have been made to this end. Tour and Barron et al.<sup>26</sup> have produced graphene nanosheets in ortho-dichlorobenzene (ODCB) and then used alkyl iodides to covalently functionalize graphene in ODCB dispersions. Haddon et al.<sup>27</sup> and Tour et al.<sup>28</sup> have functionalized graphene by treatment with aryl diazonium salts. Yan et al.<sup>29</sup> have covalently immobilized graphene on silicon wafers with perfluorophenylazide (PFPA) as the coupling agent. Besides, some other reports achieved this goal in an alternative way—first prepare functionalized GO and then reduce them to functionalized graphene. For instance, Niu et al.<sup>30</sup> functionalized graphene sheets covalently with biocompatible poly-L-lysine (PLL) by the reactions of epoxy groups on GO and amino groups on PLL followed by reduction of GO with  $NaBH_4$ . Salavagione et al.<sup>31</sup> produced poly(vinyl alcohol) (PVA) modified graphene through esterification of the carboxylic groups on GO and the hydroxyl groups of PVA and subsequent reduction of GO with hydrazine. Despite these efforts, however, there are no reports yet about the scalable functionalization of graphene by a simple and general method. On the other hand, it is extremely easy for graphene or GO to assemble into clusters or aggregates during functionalization or chemical reducing

because of the strong interactions between flat sheets, posing a big challenge for accessing individually dispersed functionalized graphene nanosheets (f-GNs). Hence, AFM images of single f-GNs have been hardly gained and rarely shown in the literature. This is different from the case of CNTs, in which individually functionalized CNTs are hard to aggregate again into bundles because of their small contacting area of cylindrical topology. Therefore, the methods used to functionalize CNTs could only shed light for the functionalization of graphene rather than promise the success of such a modification, especially for the target of single f-GNs.

To meet the challenges, herein, we report a sufficient strategy to synthesize single f-GNs readily based on the powerful nitrene chemistry. The nitrenes are highly reactive intermediates that can be generated from azide groups through either thermolysis or irradiation, which has been tried for the covalent functionalization of CNTs,<sup>32–36</sup> fullerenes,<sup>37–39</sup> carbon nanoions,<sup>40</sup> exfoliated graphite<sup>41</sup> and epitaxial graphene<sup>42</sup> via the [2 + 1] cycloaddition of nitrenes to the  $\pi$ -electron system. In this paper, we utilize a series of compounds containing azide groups to introduce various functional groups or polymeric chains onto graphene nanosheets via the nitrene cycloaddition. This strategy has considerable advantages compared with the previous reports. First, this is a general methodology that can be used to prepare many kinds of f-GNs. For example, various functional groups (e.g.,  $-OH$ ,  $-COOH$ ,  $-NH_2$ , and  $-Br$ ), alkyl chains and polymers (e.g., poly(ethylene glycol) (PEG), polystyrene (PS)) can be covalently anchored on graphene in one step with the same protocol. Second, the largely obtainable GO is used as the graphene precursor and the synthesis procedure is convenient since the reduction of GO to graphene and the nitrene cycloaddition are proceed simultaneously, enabling the production of f-GNs easily scalable. Third, the obtained f-GNs are really single sheets as demonstrated by AFM measurements, opening the door for the facile fabrication of individually dispersed f-GNs with good solubility and processability in desired solvents such as chloroform and toluene. Fourth, the f-GNs, contrary to ordinary surmising, are highly electrically conductive, ironing out the

- (24) Dreyer, D. R.; Park, S.; Bielawski, C. W.; Ruoff, R. S. *Chem. Soc. Rev.* **2010**, *39*, 228–240.  
(25) Tasis, D.; Tagmatarchis, N.; Bianco, A.; Prato, M. *Chem. Rev.* **2006**, *106*, 1105–1136.  
(26) Hamilton, C. E.; Lomeda, J. R.; Sun, Z. Z.; Tour, J. M.; Barron, A. R. *Nano Lett.* **2009**, *9*, 3460–3462.  
(27) Bekyarova, E.; Itkis, M. E.; Ramesh, P.; Berger, C.; Sprinkle, M.; de Heer, W. A.; Haddon, R. C. *J. Am. Chem. Soc.* **2009**, *131*, 1336–1337.  
(28) Lomeda, J. R.; Doyle, C. D.; Kosynkin, D. V.; Hwang, W. F.; Tour, J. M. *J. Am. Chem. Soc.* **2008**, *130*, 16201–16206.  
(29) Liu, L.; Yan, M. *Nano Lett.* **2009**, *9*, 3375–3378.  
(30) Shan, C. S.; Yang, H. F.; Han, D. X.; Zhang, Q. X.; Ivaska, A.; Niu, L. *Langmuir* **2009**, *25*, 12030–12033.  
(31) Salavagione, H. J.; Gomez, M. A.; Martinez, G. *Macromolecules* **2009**, *42*, 6331–6334.

- (32) Holzinger, M.; Vostrowsky, O.; Hirsch, A.; Hennrich, F.; Kappes, M.; Weiss, R.; Jellen, F. *Angew. Chem., Int. Ed.* **2001**, *40*, 4002–4005.  
(33) Holzinger, M.; Abroha, J.; Whelan, P.; Graupner, R.; Ley, L.; Hennrich, F.; Kappes, M.; Hirsch, A. *J. Am. Chem. Soc.* **2003**, *125*, 8566–8580.  
(34) Holzinger, M.; Steinmetz, J.; Samaille, D.; Glerup, M.; Paillet, M.; Bernier, P.; Ley, L.; Graupner, R. *Carbon* **2004**, *42*, 941–947.  
(35) Wang, G. J.; Dong, Y.; Liu, L.; Zhao, C. X. *J. Appl. Polym. Sci.* **2007**, *105*, 1385–1390.  
(36) Gao, C.; He, H.; Zhou, L.; Zheng, X.; Zhang, Y. *Chem. Mater.* **2009**, *21*, 360–370.  
(37) Averdung, J.; Mattay, J. *Tetrahedron* **1996**, *52*, 5407–5420.  
(38) Yashiro, A.; Nishida, Y.; Ohno, M.; Eguchi, S.; Kobayashi, K. *Tetrahedron Lett.* **1998**, *39*, 9031–9034.  
(39) Nakahodo, T.; Okada, M.; Morita, H.; Yoshimura, T.; Ishitsuka, M. O.; Tsuchiya, T.; Maeda, Y.; Fujihara, H.; Akasaka, T.; Gao, X.; Nagase, S. *Angew. Chem., Int. Ed.* **2008**, *47*, 1298–1300.  
(40) Zhou, L.; Gao, C.; Zhu, D.; Xu, W.; Chen, F. F.; Palkar, A.; Echeugoyen, L.; Kong, E. S. *Chem.—Eur. J.* **2009**, *15*, 1389–1396.  
(41) Strom, T. A.; Dillon, E. P.; Hamilton, C. E.; Barron, A. R. *Chem. Commun.* **2010**. DOI:10.1039/c001488e.  
(42) Choi, J.; Kim, K.; Kim, B.; Lee, H.; Kim, S. *J. Phys. Chem. C* **2009**, *113*, 9433–9435.

widely accepted misunderstanding that chemical functionalization would destroy the conjugated network of graphene and make properties such as conductivity loss intrinsic, and thus promising unlimited application of f-GNs.

The resulting diversiform f-GNs have a broad scope of potential applications because of their excellent properties, which include the use as substrates for depositing of inorganic nanoparticles (e.g., noble metal nanoparticles for heterogeneous catalysis, magnetic nanoparticles for separation and magnetic resonance imaging, etc.), as well-dispersible and conductive nanofillers in polymer matrix to fabricate high-performance graphene-polymer composites, as components in electronics devices, as platforms for devising other graphene-based nanomaterials with designated properties by reactions on the surface reactive moieties of f-GNs, and so forth.

### Experimental Section

**Materials.** Graphene oxide (GO) was synthesized from natural graphite powder (40  $\mu\text{m}$  in size, Qingdao Henglide Graphite Co., Ltd.) using a modified Hummers method.<sup>43,44</sup> Sodium azide (99%), poly(ethylene glycol) monomethyl ether (PEG-OH with  $M_n = 350, 750,$  and  $1900$  g/mol), 1,3-dicyclohexylcarbodiimide (DCC, 98%), *N,N*-(dimethylamino)pyridine (DMAP, 98%), 2-bromoisobutyl bromide (98%), *N,N,N',N'',N'''*-pentamethyldiethylenetriamine (PMDETA, 99%), anhydrous iron(III) chloride ( $\text{FeCl}_3$ , 98%), and diethylene glycol (DEG, 99%) were purchased from Alfa Aesar and used as received.  $\epsilon$ -Caprolactone (Acros, 99%) and palmitoyl chloride (Fluke, 97%) were used without further purification. Ethylene glycol (99%) and stannous octoate ( $[\text{CH}_3(\text{CH}_2)_3\text{CH}(\text{C}_2\text{H}_5)\text{COO}]_2\text{Sn}$ , 95%) were purchased from Aldrich and used as received. 2-Chloroethanol (99%), 3-chloropropylamine hydrochloride (98%), palmitic acid (97%), *N*-methyl-2-pyrrolidinone (NMP), acetone, tetrahydrofuran (THF), *N,N*-dimethyl formamide (DMF), dimethylsulfoxide (DMSO), and other solvents were obtained from Sinopharm Chemical Reagent Co., Ltd. and used as received. Dichloromethane ( $\text{CH}_2\text{Cl}_2$ ) and triethylamine (TEA) were dried with  $\text{CaH}_2$  and distilled under reduced pressure before use. Styrene (Alfa Aesar, 98%) was purified twice by passing the monomers through a column filled with basic alumina to remove the inhibitor. CuBr (Aldrich, 98%) was obtained from Aldrich and purified according to the published procedures.<sup>45</sup> 2-Azidoethanol (Az-OH), 3-azidopropan-1-amine (Az-NH<sub>2</sub>), 4-(2-azidoethoxy)-4-oxobutanoic acid (Az-COOH), and 2-azidoethyl-2-bromo-2-methylpropanoate (Az-Br) were prepared according to the previous procedures.<sup>36</sup> Azido-terminated polystyrene (Az-PS) with  $M_n = 2,515$  g/mol and  $M_w/M_n = 1.20$  was synthesized according to previous reports<sup>46,47</sup> with Az-Br as the ATRP initiator. Azido-terminated long alkyl chain (Az-C16) and azido-terminated poly(ethylene glycol) (Az-PEG) were prepared according to the previous procedures<sup>48</sup> and the details are given in the Supporting Information.

**Instrument.** Atomic force microscopy (AFM) was done using a Digital Instrument Nanoscope IIIa scanning probe microscope, operating at the tapping mode, with samples prepared by spin-coating sample solutions onto freshly cleaved mica substrates at 1500 rpm. Transmission electron microscopy (TEM) analysis was performed on a JEOL JEM2010 electron microscope at 200 kV, or a FEI/Philips CM200 electron microscope operating at 160 kV. Scanning electron microscopy (SEM) images were obtained on a Hitachi S4800 field-emission SEM system. The X-ray diffractions (XRD) were recorded on a Philips X'Pert PRO diffractometer equipped with Cu K $\alpha$  radiation (40 kV, 40 mA). X-ray photoelectron spectroscopy (XPS) were performed with a RBD upgraded PHI-5000C ESCA system (Perkin-Elmer) with Mg K $\alpha$  radiation ( $h\nu = 1253.6$  eV) at a power of 250 W. Raman spectra were collected on a Jobin-Yvon LabRam HR 800 Raman spectroscopy equipped with a 514.5 nm laser source. Thermal gravimetric analysis (TGA) was carried out on a Perkin-Elmer Pyris 6 TGA instrument with a heating rate of 20  $^\circ\text{C}/\text{min}$  under a nitrogen flow (30 mL/min). Gel permeation chromatography (GPC) was recorded on PL GPC 50 plus instrument. Fourier-transform infrared (FTIR) spectra were recorded on a Bruker Vector 22 spectrometer (KBr disk). Conductivity was measured using a four-probe resistivity instrument (RTS-4, PROBES TECH).

**Preparation of Functionalized Graphene Nanosheets (f-GNs).** Typically, GO (50 mg) and NMP (20 mL) were placed in a 50 mL Schlenk flask fitted with a condenser. The mixture was treated with an ultrasonic bath (40 kHz) for 1 h and then placed on a magnetic stirrer with an oil bath. After the mixture was bubbled with nitrogen for 30 min, a given amount (e.g., 1.0 g) of azide compounds (e.g., Az-OH, Az-COOH, Az-NH<sub>2</sub>, Az-Br, Az-C16, Az-PEG, Az-PS) was added. The reaction mixture was then heated and maintained around 160  $^\circ\text{C}$  in a nitrogen atmosphere under constant stirring for 18 h. After being cooled to room temperature, the mixture was separated by repeated centrifugation and washed with acetone and/or DMF, affording the final product of f-GNs (coded as G-N-OH, G-N-COOH, G-N-NH<sub>2</sub>, G-N-Br, G-N-C16, G-N-PEG, G-N-PS, respectively).

**Synthesis of G-N-OH-g-PCL by Ring-Opening Polymerization (ROP).** G-N-OH (10 mg) was dispersed via sonication in DMF (5 mL).  $\epsilon$ -Caprolactone (6.0 g) and stannous octoate (2 mg) were added under a nitrogen atmosphere. The reaction was allowed to proceed for 24 h at 120  $^\circ\text{C}$  under constant stirring. The product was separated by centrifugation and washed with DMF.

**Synthesis of G-N-NH<sub>2</sub>-g-C16 by Amidation.** G-N-NH<sub>2</sub> (10 mg) was dispersed via sonication in dried chloroform (8 mL). After dried TEA (1.75 g) and palmitoyl chloride (1.5 g) were added, the reaction was allowed to proceed at room temperature for 24 h under constant stirring. The product was separated by centrifugation and washed in turn with 1 M HCl, deionized water, and acetone.

**Synthesis of G-N-Br-g-PS by Atom Transfer Radical Polymerization (ATRP).** G-N-Br (10 mg) was dispersed via sonication in DMF (5 mL). Styrene (5.2 g), CuBr (14.4 mg) and PMDETA (21  $\mu\text{L}$ ) were added under a nitrogen atmosphere. The reaction was allowed to proceed for 24 h at 80  $^\circ\text{C}$  under constant stirring. The product was separated by centrifugation and washed with DMF.

**Preparation of G-N-COOH-Fe<sub>3</sub>O<sub>4</sub> Nanohybrids.** Typically, NaOH (200 mg) was added in DEG (20 mL) and heated at 120  $^\circ\text{C}$  for 1 h in a nitrogen atmosphere, and cooled down and

(43) Kovtyukhova, N. I.; Ollivier, P. J.; Martin, B. R.; Mallouk, T. E.; Chizhik, S. A.; Buzaneva, E. V.; Gorchinskiy, A. D. *Chem. Mater.* **1999**, *11*, 771–778.

(44) Tung, V. C.; Allen, M. J.; Yang, Y.; Kaner, R. B. *Nanotechnol.* **2009**, *4*, 25–29.

(45) Cheng, G. L.; Boker, A.; Zhang, M. F.; Krausch, G.; Muller, A. H. E. *Macromolecules* **2001**, *34*, 6883–6888.

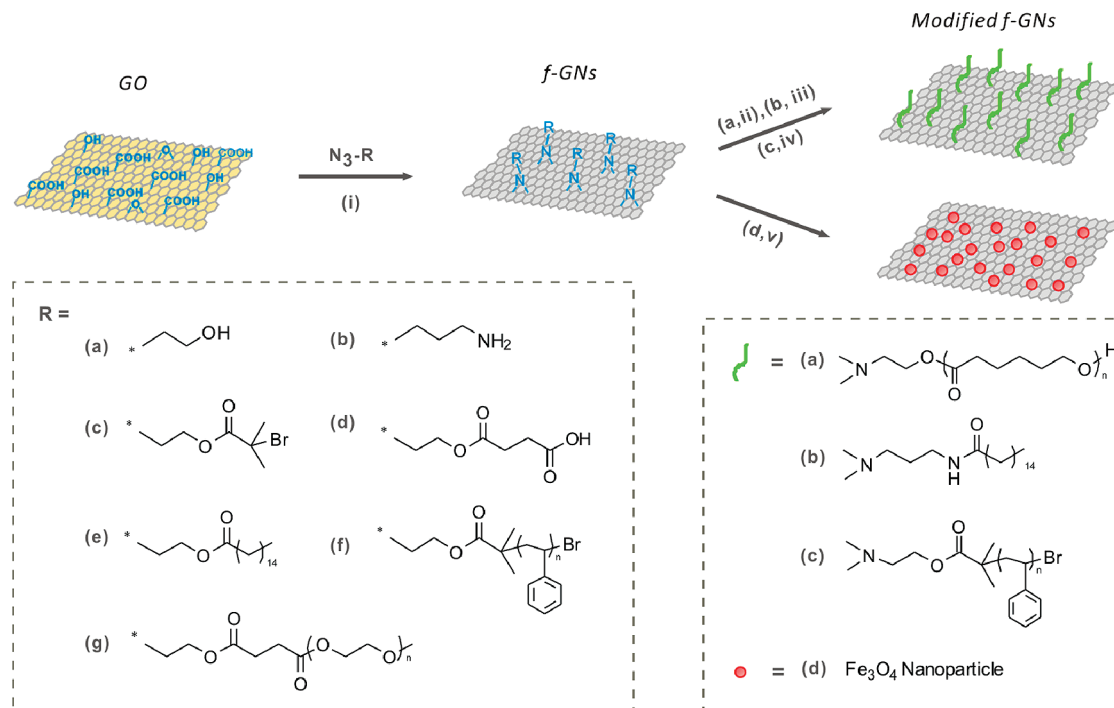
(46) Tsarevsky, N. V.; Sumerlin, B. S.; Matyjaszewski, K. *Macromolecules* **2005**, *38*, 3558–3561.

(47) Gao, H. F.; Matyjaszewski, K. *J. Am. Chem. Soc.* **2007**, *129*, 6633–6639.

(48) Wu, J.; Gao, C. *Macromol. Chem. Phys.* **2009**, *210*, 1697–1708.



**Scheme 1. General Strategy for the Preparation of Functionalized Graphene Nanosheets (f-GNs) by Nitrene Chemistry and the Further Chemical Modifications<sup>a</sup>**



<sup>a</sup> Reagents and conditions: (i) NMP, 160 °C, 18 h; (ii)  $\epsilon$ -caprolactone, stannous octoate, 120 °C, 24 h; (iii) palmitoyl chloride, TEA, r.t., 24 h; (iv) styrene, CuBr/PMDETA, 80 °C, 24 h; (v) FeCl<sub>3</sub>, NaOH, DEG, 220 °C, 1 h.

kept at 70 °C to produce a NaOH/DEG stock solution (10 mg NaOH/mL). G-N-COOH (30 mg) was dispersed via sonication in DEG (20 mL), and sonicated for 1 h. Then FeCl<sub>3</sub> (120 mg) was added and stirred for 1 h. The above mixture was heated to 220 °C for 30 min under the protection of nitrogen flow and constant stirring. A NaOH/DEG stock solution (5 mL) was injected rapidly into the above hot mixture. The resulting mixture was further heated at 220 °C for 1 h. The final product was separated by centrifugation and washed with ethanol.

**Preparation of f-GNs/Polyurethane Composites.** Polyurethane was dissolved in DMF to form a 125 mg/mL polyurethane/DMF solution. A certain amount of f-GNs was dispersed in DMF by sonication and mixed with the polyurethane/DMF solution. The mixture was then spread onto a piece of glass, dried in an oven at 60 °C for 48 h, and cooled to room temperature. The glass was immersed into deionized water to allow the strip to peel off the glass. The strip was clamped between two filtered papers and dried in a vacuum at 70 °C for 12 h.

## Results and Discussion

**General Synthesis of Functionalized Graphene Nanosheets (f-GNs).** Our general strategy to f-GNs and their further chemical modifications is outlined in Scheme 1. In our methodology, various functional groups and polymers were connected onto the surfaces of graphene covalently to produce f-GNs. The functionalization is accomplished in merely a one-step reaction by simply mixing as-prepared GO and functional azides in NMP at 160 °C for 18 h. The highly reactive intermediates of nitrenes are generated upon heating the azides at elevated temperature, and some of the nitrenes are attached on the surfaces of graphene by cycloaddition with the active C=C bonds to form aziridine rings. The covalent bonding

nature between the thermally generated nitrene radicals and graphene has been verified by photoemission spectroscopy in the previous report.<sup>42</sup> At the same time, the GO is thermally reduced to graphene, causing the color of the reaction mixture to turn from light brown to dark brown and then to black, which is a sign that GO has been reduced.<sup>49</sup> By the same strategy, we have obtained many types of f-GNs with different reagents of azides, that is, hydroxyl-functionalized graphene (G-N-OH), carboxyl-functionalized graphene (G-N-COOH), amino-functionalized graphene (G-N-NH<sub>2</sub>), and bromine-functionalized graphene (G-N-Br), long alkyl chain-functionalized graphene (G-N-C16), polystyrene-functionalized graphene (G-N-PS), and poly(ethylene glycol)-functionalized graphene (G-N-PEG). To test whether the functional groups on the f-GNs still retain their chemical activity, we conducted a series of experiments, including ring-opening polymerizations (ROP)<sup>50</sup> on G-N-OH to obtain G-N-OH-*g*-PCL, amidation on G-N-NH<sub>2</sub> to obtain G-N-NH<sub>2</sub>-*g*-C16, surface-initiated atom transfer radical polymerization (ATRP)<sup>51</sup> on G-N-Br to obtain G-N-Br-*g*-PS, and growth of metal nanoparticles on G-N-COOH to obtain G-N-COOH-Fe<sub>3</sub>O<sub>4</sub> nanohybrids. All of these objectives have been achieved, demonstrating that the f-GNs with functional groups are able to undergo further chemical modifications. The f-GNs and further chemically modified f-GNs were fully characterized by various measurements and the results will be given and discussed in the following text.

(49) Williams, G.; Seger, B.; Kamat, P. V. *ACS Nano* **2008**, *2*, 1487–1491.

(50) Wang, K.; Li, W. W.; Gao, C. *J. Appl. Polym. Sci.* **2007**, *105*, 629–640.

(51) Matyjaszewski, K.; Xia, J. *Chem. Rev.* **2001**, *101*, 2921–2990.

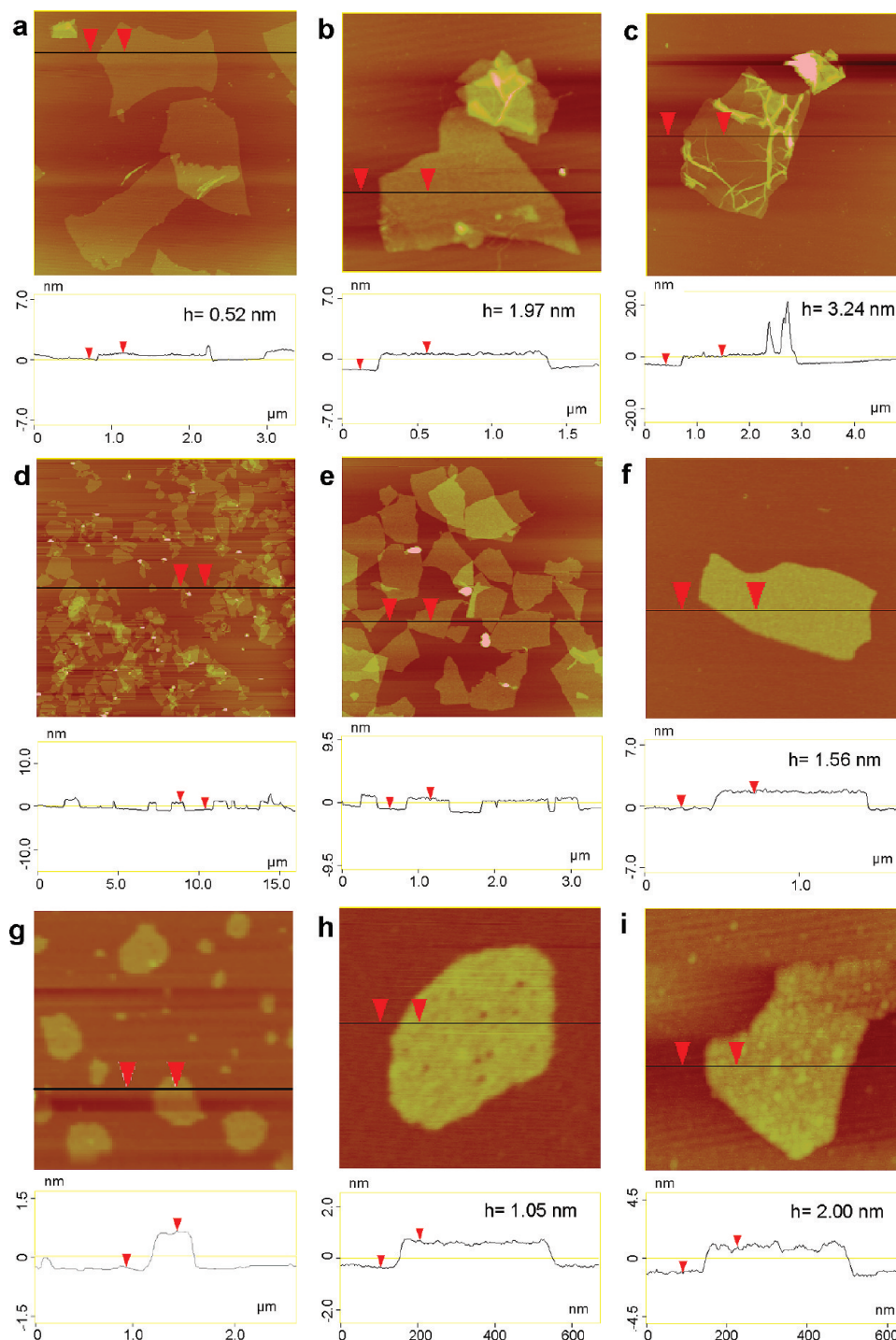


**Figure 1.** AFM images of (a) GO, (b) G-N-COOH, (c) G-N-Br, (d–f) G-N-C16, (g,h) G-N-PS, and (i) G-N-PEG350.

**AFM Observations.** Atomic force microscopy (AFM) is an extensively used instrumental technique that is capable of imaging and evaluating surface morphology and properties, and is also the most direct tool for the morphological characterization of graphene/GO and their derivations. By using AFM measurement, both the surface and height profiles could be accurately and easily obtained. Besides, AFM images also show whether the individual graphene sheets remain isolated or become aggregate after functionalization. Therefore, AFM images can be viewed as the most important indication that determines whether the functionalization of graphene is successfully

realized. However, there have been rare reports of AFM images of single-layered covalently functionalized graphene or GO, likely because of the extreme difficulty to achieve single sheets because of the aggregation of graphene during the reaction.

Here, we successfully obtained many AFM images of f-GNs by spin-coating the as-prepared samples solutions on freshly cleaved mica substrates under the tapping mode. Figure 1 and Figure S1 (see the Supporting Information) show typical AFM images of part f-GNs with the corresponding height profiles. The AFM images of all of the samples display single-layer graphene sheets with

lateral dimensions of several micrometers, demonstrating the individual graphene sheets remain isolated after being modified with various compounds. The heights of f-GNs are in the range of 1–3 nm, which is obviously higher than that of pristine GO or graphene because of the introduction of functional moieties on f-GNs. For G-N-OH, G-N-COOH, G-N-NH<sub>2</sub>, G-N-Br, and G-N-C16, the surfaces are smooth or with a few wrinkles and folds. For G-N-PEG and G-N-PS, the surfaces are relatively coarse and a lot of spherical protuberances appear on the surfaces of graphene evenly, which are formed by the intertangling of neighboring polymer chains anchored on the f-GNs. Thus, the covalent graphene-polymer conjugates were successfully prepared via the one-step “grafting to” approach, which is an alternative to the “grafting from” approach that generally needs multistep process to graft polymer chains from graphene or GO.<sup>52–54</sup> In addition, because well-defined polymers with designable molecular weights and architectures can be synthesized by ATRP,<sup>55</sup> and the terminal bromine of polymers can be easily converted into azide,<sup>56–58</sup> a myriad of polymer-functionalized graphene could be easily obtained taking advantage of the combination of ATRP and nitrene chemistry. This kind of graphene-polymer structures can be regarded as two-dimensional (2D) macromolecular brushes, which can be used as building blocks or coatings for construction of large-area surface brushes in the applications of water-based lubrication and surface-wetting.<sup>59</sup>

It can be also seen from the AFM images that the individual graphene nanosheets mostly still maintained the separated single layers. This is, to our knowledge, the first report of AFM images of many single-sheets of covalently functionalized graphene. This result also in turn indicates the great superiority and reliability of our functionalization methodology, because the single-layer functionalized graphene is very difficult to obtain in both quality and quantity by any other previously reported methods. In addition, the single-layer distribution state prevents the aggregation of functionalized graphene, which will greatly facilitate the further visualization, manipulation, modification, and applications of the f-GNs.

**SEM and TEM Observations.** Scanning electron microscopy (SEM) and transmission electron microscopy (TEM) observations were also undertaken to characterize the nanoscale morphologies of the f-GNs. The SEM images of selected samples are shown in Figure 2 and Figure S2 (see the Supporting Information). Graphite

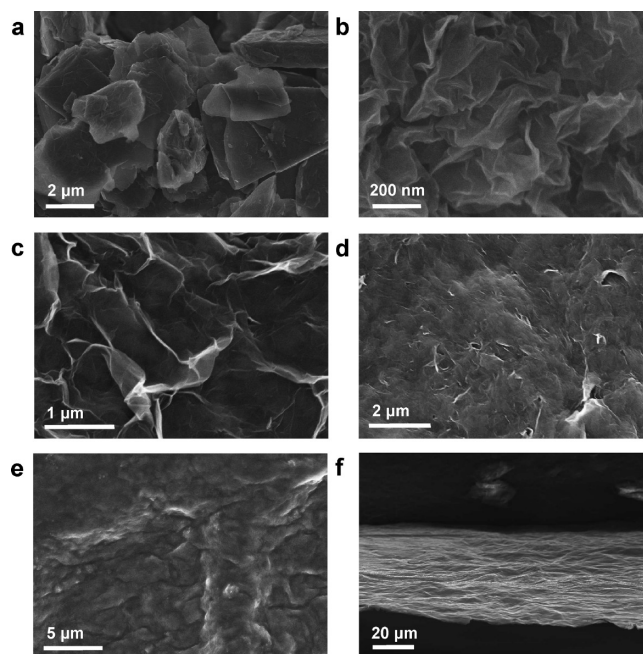


**Figure 2.** SEM top-view images of (a) graphite, (b) GO, (c) G-N-OH, (d) G-N-PS, and (e) G-N-C16, and (f) SEM side-view image of a filtered film of G-N-C16.

appears to be piled up with thick cakes, while GO is exfoliated into thin large flakes with wavy wrinkles. The f-GNs are mostly wrinkled flakes that are similar with GO, but for the f-GNs functionalized with long chains and polymers (G-N-C16, G-N-PS, and G-N-PEG), the surfaces are coarse and hairy, and the edges of the flakes are blurry. Besides, the SEM side-view images of a filtered film of G-N-C16 (Figure 2f) and some other f-GNs (see Figure S2 in the Supporting Information) all display a layered-stacking structure of thin graphene sheets. It is worth mentioning that because GO is insulated, before conducting SEM measurements, the sample has to be coated with a thin conductive film by sputtering with Au to minimize charging effects. Conversely, the f-GNs could be directly characterized by SEM without additional treatments, which reveals that f-GNs are conductive resulting from the thermal reduction of GO.

Figure 3 and Figure S3 (see the Supporting Information) show the bright-field TEM images of representative samples. The TEM samples are prepared by placing a drop of diluted dispersion onto holey carbon grids. GO has a typical shape resembling the large crumpled thin flake, and the morphology f-GNs did not change significantly after functionalization. Because the inorganic nanoparticles can be used for the site identification of carboxyl groups of nanocarbons,<sup>60</sup> we clarify the location of the functional groups on G-N-COOH by in situ growth of Fe<sub>3</sub>O<sub>4</sub> nanoparticles. The X-ray diffraction (XRD) and energy-dispersive spectrometer (EDS) measurements for the resulting G-N-COOH-Fe<sub>3</sub>O<sub>4</sub> confirmed the presence of Fe<sub>3</sub>O<sub>4</sub> nanoparticles, and the magnetic G-N-COOH-Fe<sub>3</sub>O<sub>4</sub> dispersed in DMF could be easily separated by an

(52) Fang, M.; Wang, K.; Lu, H.; Yang, Y.; Nutt, S. *J. Mater. Chem.* **2010**, *20*, 1982–1992.

(53) Lee, S. H.; Dreyer, D. R.; An, J.; Velamakanni, A.; Piner, R. D.; Park, S.; Zhu, Y.; Kim, S. O.; Bielawski, C. W.; Ruoff, R. S. *Macromol. Rapid Commun.* **2009**, *31*, 281–288.

(54) Yang, Y.; Wang, J.; Zhang, J.; Liu, J.; Yang, X.; Zhao, H. *Langmuir* **2009**, *25*, 11808–11814.

(55) Matyjaszewski, K.; Tsarevsky, N. V. *Nat. Chem.* **2009**, *1*, 276–288.

(56) Gao, H.; Matyjaszewski, K. *Macromolecules* **2006**, *39*, 4960–4965.

(57) Golas, P. L.; Matyjaszewski, K. *Chem. Soc. Rev.* **2010**, *39*, 1338–1354.

(58) Coessens, V.; Pintauer, T.; Matyjaszewski, K. *Prog. Polym. Sci.* **2001**, *26*, 337–377.

(59) Klein, J.; Kumacheva, E.; Mahalu, D.; Perahia, D.; Fetters, L. J. *Nature* **1994**, *370*, 634–636.

(60) Yuge, R.; Zhang, M.; Tomonari, M.; Yoshitake, T.; Iijima, S.; Yudasaka, M. *ACS Nano* **2008**, *2*, 1865–1870.



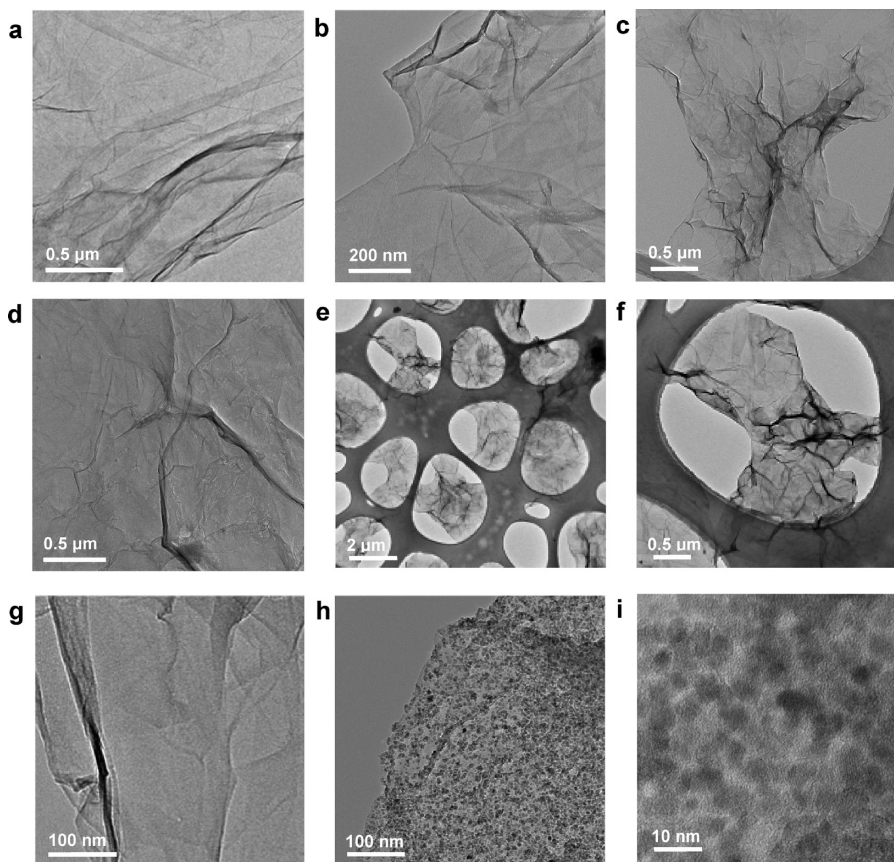


**Figure 3.** TEM images of (a) GO, (b) G-N-OH, (c) G-N-PS, (d) G-N-PEG750, (e, f) G-N-OH-g-PCL, (g) G-N-COOH, and (h, i) G-N-COOH-Fe<sub>3</sub>O<sub>4</sub>.

external magnetic field (see Figure S4 in the Supporting Information). The TEM images of G-N-COOH-Fe<sub>3</sub>O<sub>4</sub> nanocomposite in Figure 3h,i and Figure S5a–c (see the Supporting Information) show that the nanosheets of G-N-COOH are evenly decorated by Fe<sub>3</sub>O<sub>4</sub> nanoparticles with average size of 3 nm in diameter. In comparison, Fe<sub>3</sub>O<sub>4</sub> nanoparticles could not generate on G-N-OH (see Figure S5d–f in the Supporting Information). These results demonstrate that the carboxyl groups are uniformly linked on the entire surfaces of G-N-COOH, whereas there is almost no carboxyl group on G-N-OH, implying that (1) the originally uncertain and unstable functional groups on GO had been removed completely during the high-temperature reaction, and (2) the prospective sole type of functional groups were freshly immobilized onto f-GNs. The exclusive character of reactive groups is crucial for the further modification of graphene to control the surface functionality and properties.

**TGA Results and Functional Group Density of f-GNs.** The thermal behaviors of selected samples were recorded by thermal gravimetric analysis (TGA) in the nitrogen atmosphere (Figure 4). The graphite has a very high thermal stability and has a weight loss of only 1.1% at 600 °C because of the decomposing and volatilizing of some impurity. The weight loss curves of f-GNs (Figure 4a–c) exhibit an obvious step of mass loss before 500 °C, which arise from organic compounds grafted from/to the f-GNs. Therefore, the amounts of grafted organic compounds on f-GNs can be calculated from their TGA data, and the

degree of functionalization of graphene can be also easily obtained accordingly. Taking G-N-OH as an example, it has a weight loss of 20.9%, which corresponds to 3.54 mmol hydroxyl-terminated group per gram of G-N-OH, or 53.7 functional groups per 1000 carbons of graphene, or one functional group per 18.6 carbon atoms (or 0.5 nm<sup>2</sup>) of graphene. The data calculated from TGA curves of all the f-GNs samples are listed in Table 1. The degrees of functionalization of f-GNs are close to or larger than those previously reported for the functionalized CNTs<sup>36,61</sup> and f-GNs,<sup>28</sup> and the high values indicate the efficient nitrene functionalization on graphene. The extrapolated onset temperatures of thermal decomposition of f-GNs are in the range of 256–343 °C (see Table 1), which is higher than that of GO (155 °C) by about 100–190 °C, suggesting f-GNs have much better thermal stability compared to GO.

In addition, the weight loss of hydrazine treated G-N-OH (r-G-N-OH) is almost the same as that of G-N-OH, while the weight loss of hydrazine-treated GO (r-GO) is obviously lower than that of GO (Figure 4a), illustrating the hydroxyl groups on G-N-OH could survive the hydrazine reduction and have higher chemical stability than the oxygen-containing groups on GO, which might benefit from the aziridine rings on f-GNs formed by the nitrene cycloadditions that link between the functional

(61) Gao, C.; Vo, C. D.; Jin, Y. Z.; Li, W. W.; Armes, S. P. *Macromolecules* **2005**, *38*, 8634–8648.

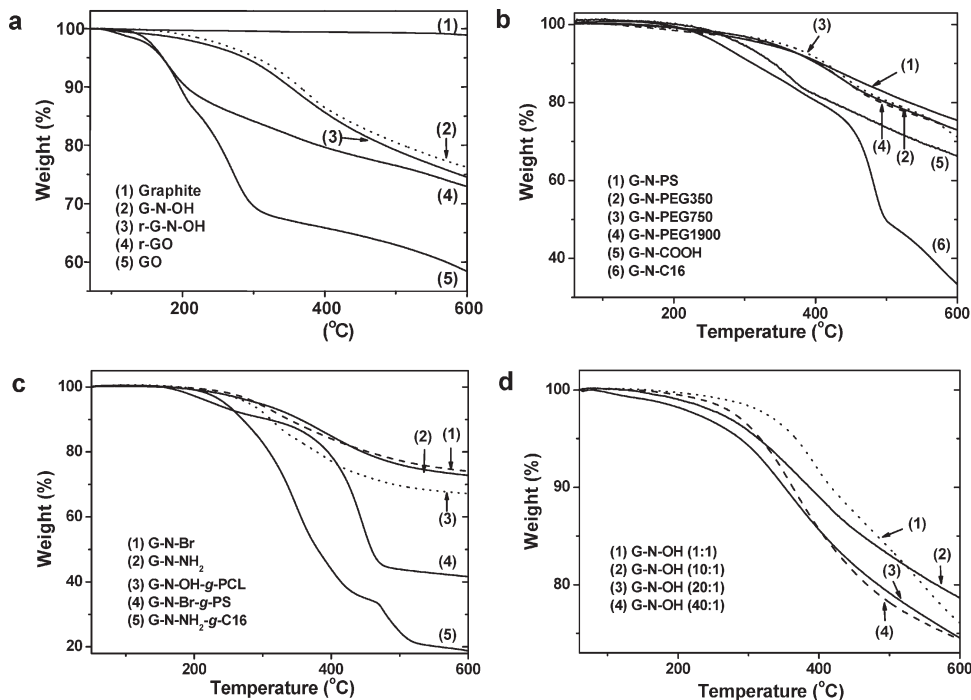


**Figure 4.** TGA curves of representative samples. (a) Graphite (1), G-N-OH (2), r-G-N-OH (3), r-GO (4), and GO (5). (b) G-N-PS (1), G-N-PEG350 (2), G-N-PEG750 (3), G-N-PEG1900 (4), G-N-COOH (5), and G-N-C16 (6). (c) G-N-Br (1), G-N-NH<sub>2</sub> (2), G-N-OH-g-PCL (3), G-N-Br-g-PS (4), and G-N-NH<sub>2</sub>-g-C16 (5). (d) G-N-OH(1:1) (1), G-N-OH(10:1) (2), G-N-OH(20:1) (3), and G-N-OH(40:1) (4).

**Table 1.** Data Obtained from TGA Curves and Electrical Conductivities of f-GNs

samples	$f_w^a$ (%)	concn <sup>b</sup> (mmol/g)	density			$T_d^f$ (°C)	conductivity <sup>g</sup> (S/m)
			$d_f^c$	$d_{\text{carbon}}^d$	$d_{\text{area}}^e$ (nm <sup>2</sup> )		
GO	37.1					155	$2 \times 10^{-5}^\dagger$
G-N-OH	20.9	3.54	53.7	18.6	0.5	270	0.3*
G-N-COOH	26.4	1.66	27.1	36.9	0.9	278	2*
G-N-NH <sub>2</sub>	23.9	3.31	52.3	19.1	0.5	277	0.2*
G-N-Br	22.6	1.09	16.9	59.3	1.5	256	30*
G-N-C16	50.2	1.69	40.7	24.6	0.6	276	0.1
G-N-PS	17.6	0.07	1.0	980	24.5	288	370
G-N-PEG350	20.0	0.41	6.1	163	4.1	318	270
G-N-PEG750	19.5	0.22	3.3	307	7.7	343	580
G-N-PEG1900	20.6	0.10	1.5	655	16.4	338	680

<sup>a</sup> Weight loss fraction before 500 °C. <sup>b</sup> The concentration of functional groups per gram of f-GNs. <sup>c</sup> The average numbers of functional groups/chains per 1000 carbons of graphene occupied. <sup>d</sup> The average numbers of carbon atoms of graphene per functional group/chain occupied. <sup>e</sup> The average areas of graphene per functional group/chain occupied. <sup>f</sup> The extrapolated onset temperature of thermal decomposition. <sup>g</sup> Electrical conductivities of free-standing paper samples of f-GNs. The “\*” indicates that the conductivity is recorded on a thin film of 10 wt % f-GNs/polyurethane composites. The “†” indicates that the data are taken from ref 54.

groups and graphene. The weight losses of G-N-OH-g-PCL, G-N-Br-g-PS, and G-N-NH<sub>2</sub>-g-C16 (Figure 4c) are much larger than their corresponding precursors of G-N-OH, G-N-Br, and G-N-NH<sub>2</sub>, respectively, suggesting the successful surface chemical modifications. The TGA curves of G-N-OH of parallel experiments with different feed ratios in Figure 4d show that the weight losses of functional groups are 16.3, 17.0, 20.9, and 21.8% for feed ratios of 1:1, 10:1, 20:1, and 40:1 (w/w), respectively. When the feed ratio was increased from 1:1 to 40:1, the functional group density rose from 2.76 to 3.69 mmol/g, revealing that the degree of functionalization of f-GNs can be adjusted to some extent by varying the feed ratio. From another point of view, 2.76 mmol/g G-N-OH (39.6 functional groups per 1000 carbons of graphene, or one group per 25.3 carbon atoms (or 0.6 nm<sup>2</sup>) of graphene)

denotes a high density of hydroxyl groups already, indicating the high efficiency of our strategy because the feed ratio as low as 1:1 was adopted.

**XPS and FTIR Spectra.** X-ray photoelectron spectroscopy (XPS) analysis was conducted to elucidate the surface state of f-GNs with GO as the comparison, and the results are shown in Figure 5. The C 1s XPS spectrum of GO is consisted of four types of carbon: the nonoxygenated C–C (284.8 eV), the C–O (286.2 eV), the carbonyl C=O (287.8 eV), and the carboxylate O–C=O (289.0 eV).<sup>62</sup> In the C 1s XPS spectra of f-GNs, there is an additional type of carbon at 285.9 eV originating from

(62) Stankovich, S.; Dikin, D. A.; Piner, R. D.; Kohlhaas, K. A.; Kleinhammes, A.; Jia, Y.; Wu, Y.; Nguyen, S. T.; Ruoff, R. S. *Carbon* **2007**, *45*, 1558–1565.



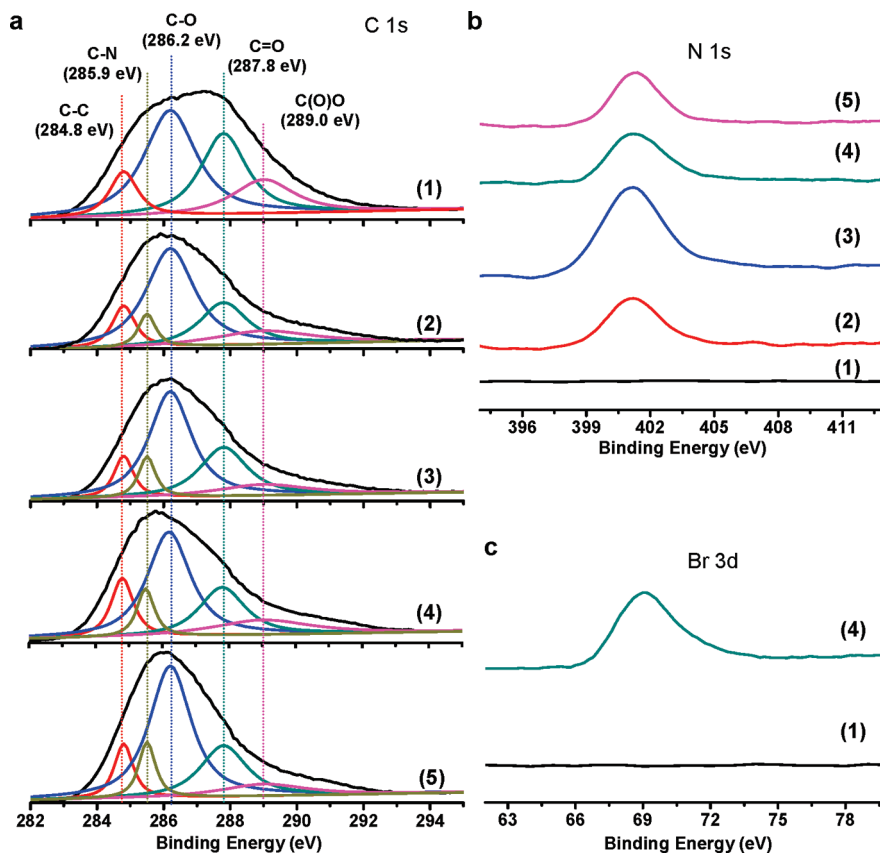


**Figure 5.** XPS spectra of GO (1), G-N-OH (2), G-N-NH<sub>2</sub> (3), G-N-Br (4), and G-N-COOH (5): (a) the carbon 1s region, (b) the nitrogen 1s region, and (c) the bromine 3d region.

C–N. The obvious N 1s peaks at 401 eV in the XPS spectra of f-GNs (Figure 5b) confirm the existence of nitrogen-containing groups on f-GNs, while no N 1s signal is detected in GO. The relative atomic ratios of N/C are 3.73, 2.83, 2.37, and 6.65% for G-N-OH, G-N-COOH, G-N-Br, and G-N-NH<sub>2</sub>, respectively. It is worth noting that the N/C of G-N-NH<sub>2</sub> is about twice those of the other f-GNs, which is reasonable because there are two nitrogen atoms in each of the functional moiety on G-N-NH<sub>2</sub> (one from the aziridine ring, the other from the amino group), although there is only one in each of the functional moiety on the other f-GNs. Besides, the Br 3d peak at 69 eV in the XPS spectra of G–N-Br also confirms the presence of bromine groups on G–N-Br. Additionally, Fourier transform infrared (FTIR) spectroscopy was also used for identifying the functional moieties on the f-GNs and chemically modified f-GNs (see Figure S6 in the Supporting Information). As a comparison, the FTIR spectra of azide-terminated compounds are shown in Figure S7 in the Supporting Information.

**XRD Patterns and Raman Spectra.** To investigate the crystal and defect structures of the synthesized f-GNs, we performed XRD measurements and Raman spectroscopy. Figure 6 shows the XRD patterns of GO and f-GNs. The (002) diffraction peak of GO is located at 10.0° (2 $\theta$ ), and the diffraction peaks of f-GNs shift to the range of 22.5–25.3°, which are close to that of pristine

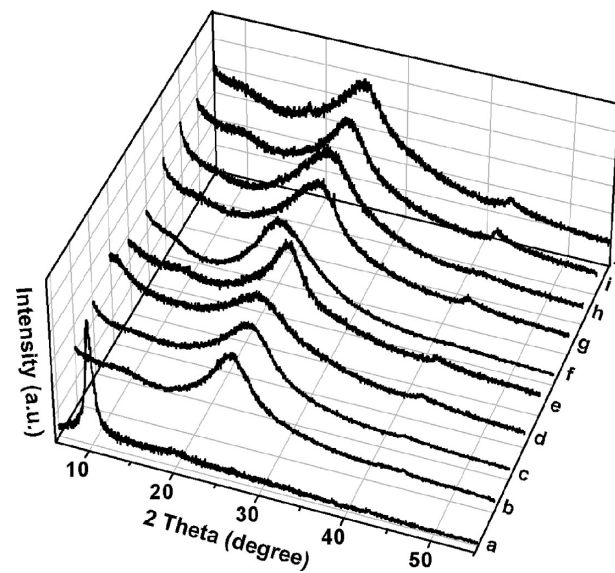


**Figure 6.** XRD patterns of (a) GO, (b) G-N-OH, (c) G-N-COOH, (d) G-N-NH<sub>2</sub>, (e) G-N-Br, (f) G-N-C16, (g) G-N-PS, (h) G-N-PEG350, (i) G-N-PEG750, and (j) G-N-PEG1900.

graphene nanosheets (26°),<sup>63</sup> revealing the reduction of graphene in f-GNs. Moreover, the (002) reflections of all the f-GNs are quite broad, which indicates that the nanosheets have poor order along the stacking direction and many free nanosheets are existed in these samples.<sup>64</sup>

(63) Wang, G. X.; Shen, X. P.; Wang, B.; Yao, J.; Park, J. *Carbon* **2009**, *47*, 1359–1364.

(64) Nethravathi, C.; Rajamathi, M. *Carbon* **2008**, *46*, 1994–1998.

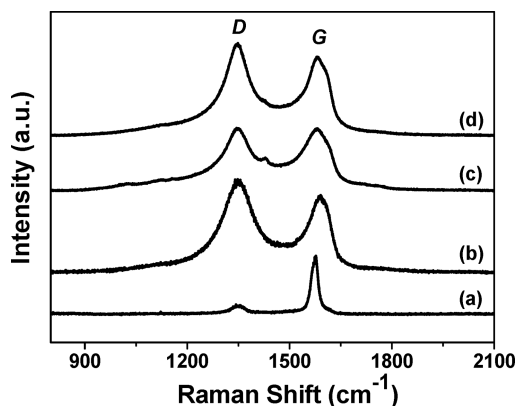


**Figure 7.** Raman spectra of (a) graphite, (b) GO, (c) G-N-COOH, and (d) G-N-Br.

The Raman spectra of graphite, GO, G-N-COOH, and G-N-Br are shown in Figure 7. Two obvious bands located at around  $1580\text{ cm}^{-1}$  and  $1350\text{ cm}^{-1}$  are observed in the Raman spectra, which are generally assigned as the G band and D band, respectively. The G band is associated with the vibration of  $\text{sp}^2$  carbon atoms in a graphitic 2D hexagonal lattice, and the D band around  $1350\text{ cm}^{-1}$  is related to the vibrations of  $\text{sp}^3$  carbon atoms of defects and disorder. By comparing the intensity of the D and G band, we can speculate the information about the disordered and ordered crystal structures of carbon. The value of  $I(D)/I(G)$  for graphite is 0.34, and it increases to 2.04 for GO due to the severe oxidation that causes many disorders in the synthesis of GO. The values of  $I(D)/I(G)$  for G-N-COOH (1.54) and G-N-Br (1.65) are smaller than that of GO but bigger than that of graphite, suggesting the orders of graphene are partly recovered in f-GNs along with the functionalization. This is also in agreement with some previous reports that demonstrated that the reduction of GO to graphene could not absolutely reduce its disorders because of the existence of some unrepaired defects,<sup>65</sup> and more numerous but smaller  $\text{sp}^2$  graphitic domains were created.<sup>66</sup>

**Solubility and Processability of f-GNs.** The as-prepared samples of f-GNs have good soluble/dispersible properties in solvents as shown in the photographs in Figure 8a. For example, G-N-OH, G-N-COOH, and G-N-PEG could be well dispersed in polar solvents such as water and DMF, G-N-C16, and G-N-PS have excellent solubility in nonpolar solvents such as chloroform and toluene, and all of the f-GNs and modified f-GNs are dispersible in DMF, NMP, DMSO, THF, and acetone. The dispersions of most f-GNs in DMF just after sonication have concentrations up to 6–8 mg/mL, which are nearly 3 orders of magnitude higher than the reported value of graphene.<sup>26</sup> The dispersions of f-GNs and modified f-GNs in various solvents are also shown in Figure S8 (see the Supporting Information). It should be noted that after being modified

with long alkyl chains, the G-N-NH<sub>2</sub> changed from hydrophilic to hydrophobic. When placed in the water/chloroform system, the G-N-NH<sub>2</sub> dispersed in the polar layer of water, whereas G-N-NH<sub>2</sub>-g-C16 transferred to the nonpolar layer of chloroform (Figure 8a), implying the successful surface modification. In comparison, the chemically reduced GO was insoluble in all of the selected solvents, and GO could not disperse in weakly polar and nonpolar solvents such as chloroform and toluene (Figure 8a and Figure S8 in the Supporting Information). The greatly improved solubility of f-GNs compared to pure graphene and reduced GO is as expected, because the latter have rare surface moieties and tend to aggregate in solvents because of the strong van der Waals interactions.<sup>67</sup>

The good solubility of the f-GNs makes them available for fabricating of composites by the convenient solution-processing technique. Herein, we produced various f-GNs/polymer films by solution phase mixing of f-GNs with polyurethane elastomer. As shown in Figure 8b, the f-GNs can form homogeneous and flexible films with polyurethane with filler weight fraction up to ca. 10%, whereas the poorly soluble reduced GO (prepared from GO by reduction with hydrazine following the published procedures<sup>68</sup>) mostly conglomerate and fracture into small fractions.

**Electrical Conductivity of f-GNs.** Electrical conductivity is one of the most important intrinsic properties of graphene. In the conventional conception, f-GNs would be much less conductive or even insulative because of the breakage of conjugation network during the conversion of  $\text{sp}^2$  into  $\text{sp}^3$  bonds. So the electrical conductivity of functionalized graphene was rarely addressed previously, and some researchers shifted their attention to noncovalent functionalization in order to keep the electrical conductivity normally “owing to the intact structure of graphene” through such a way. To clear away this riddle, we measured the conductivities of our f-GNs. Surprisingly, the f-GNs were demonstrated to be still highly conductive (Table 1). For those samples that can form free-standing films (G-N-C16, G-N-PS, G-N-PEG), the conductivities were measured on their vacuum-filtered films; while for the other samples that cannot, they were measured on their 10 wt % f-GNs/polyurethane composite films. The conductivities of f-GNs are in the range of  $1 \times 10^{-1}$  to  $1 \times 10^3\text{ S/m}$  (most of them are in the order of  $1 \times 10^2$  to  $1 \times 10^3\text{ S/m}$ ), which are less than that of polycrystalline graphite ( $125\,000\text{ S/m}$ )<sup>69</sup> but comparable to that of reduced GO ( $\sim 1 \times 10^2$  to  $1 \times 10^4\text{ S/m}$ )<sup>70</sup> and noncovalently functionalized graphene ( $\sim 1 \times 10^2\text{ S/m}$ ).<sup>71</sup> The conductivities of f-GNs/polyurethane composites are

(65) Zhou, Y.; Bao, Q. L.; Tang, L. A. L.; Zhong, Y. L.; Loh, K. P. *Chem. Mater.* **2009**, *21*, 2950–2956.

(66) Stankovich, S.; Dikin, D. A.; Piner, R. D.; Kohlhaas, K. A.; Kleinhammes, A.; Jia, Y.; Wu, Y.; Nguyen, S. T.; Ruoff, R. S. *Carbon* **2007**, *45*, 1558–1565.

(67) Pasricha, R.; Gupta, S.; Srivastava, A. K. *Small* **2009**, *5*, 2253–2259.

(68) Park, S.; An, J. H.; Jung, I. W.; Piner, R. D.; An, S. J.; Li, X. S.; Velamakanni, A.; Ruoff, R. S. *Nano Lett.* **2009**, *9*, 1593–1597.

(69) Wang, X.; Zhi, L. J.; Mullen, K. *Nano Lett.* **2008**, *8*, 323–327.

(70) Stankovich, S.; Dikin, D. A.; Dommett, G. H. B.; Kohlhaas, K. M.; Zimney, E. J.; Stach, E. A.; Piner, R. D.; Nguyen, S. T.; Ruoff, R. S. *Nature* **2006**, *442*, 282–286.

(71) Xu, Y.; Bai, H.; Lu, G.; Li, C.; Shi, G. *J. Am. Chem. Soc.* **2008**, *130*, 5856–5857.

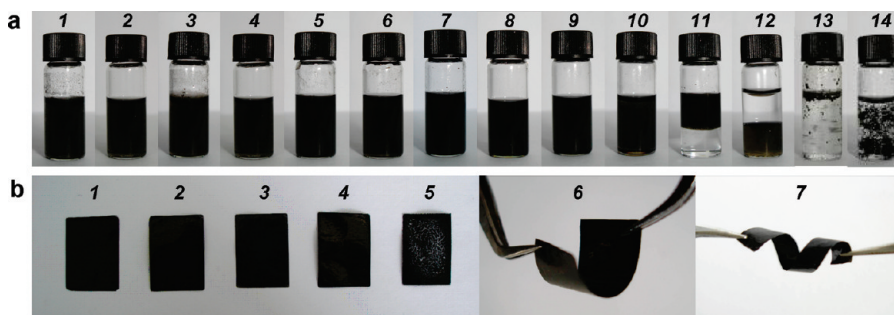


**Figure 8.** (a) Photographs of f-GNs dispersion in solvents after sonication: G-N-OH in water (1) and DMF (2), G-N-COOH in water (3) and DMF (4), G-N-PEG1900 in water (5) and DMF (6), G-N-C16 in chloroform (7) and toluene (8), G-N-PS in chloroform (9) and toluene (10), G-N-NH<sub>2</sub> in water/chloroform (11), G-N-NH<sub>2</sub>-g-C16 in water/chloroform (12), GO in chloroform (13), and reduced GO in DMF (14). (b) Photographs of 10 wt % f-GNs/polyurethane composites: (1) G-N-OH, (2) G-N-COOH, (3) G-N-NH<sub>2</sub>, (4) G-N-Br, (5) reduced GO, (6) G-N-OH, and (7) G-N-COOH.

in the range of  $1 \times 10^{-1}$  to  $1 \times 10^2$  S/m, which are comparable to those of graphene-polymer composites reported in the literature.<sup>70</sup> The improved conductivities of f-GNs as compared to GO indicate the reduction of GO in the synthesis process and the restoration of the conjugated network in f-GNs. Therefore, we can draw a conclusion that covalent functionalization may keep the conjugation network of graphene because only a small fraction of sp<sup>2</sup> bonds undergo the change into sp<sup>3</sup> ones, and thus would not impact the electrical properties of graphene considerably. The conductive functionalized graphene is promising in fabrication of novel electrical and electronic materials and devices.

### Conclusions

We have developed a facile and versatile methodology for the functionalization of graphene via nitrene chemistry. This strategy allows many kinds of functional moieties and polymers covalently bonded on graphene, resulting in functional graphene nanosheets and 2D macromolecular brushes, respectively. The functionalized graphene nanosheets mostly remained in individually separated single layers. The functional groups introduced on graphene have much better chemical and

thermal stabilities than those of GO, and can be further modified by differently chemical reactions, including surface-initiated polymerization, amidation, and reduction of metal ions. The resulting functionalized graphene nanosheets are electrically conductive, and have excellent dispersibility and processability in solvents. This general strategy can be extended to prepare many other distinctive types of functionalized graphene, opening a whole new horizon in the field of functional graphene materials.

**Acknowledgment.** This work was financially supported by the National Natural Science Foundation of China (50773038, and 20974093), National Basic Research Program of China (973 Program) (2007CB936000), the Fundamental Research Funds for the Central Universities (2009QNA4040), Qianjiang Talent Foundation of Zhejiang Province (2010R10021), and the Foundation for the Author of National Excellent Doctoral Dissertation of China (200527).

**Supporting Information Available:** Additional experimental details, AFM, SEM and TEM images, FTIR spectra, GPC curve; XRD, EDS, and photographs of G-N-COOH-Fe<sub>3</sub>O<sub>4</sub>; and photographs of GO, f-GNs, modified f-GNs, and reduced GO in various solvents (PDF). This material is available free of charge via the Internet at <http://pubs.acs.org>.